Floquet Modal Analysis to Detect Cracks in a Rotating Shaft on Anisotropic Supports

Matthew S. Allen[1] and Jerry H. Ginsberg[2]
[1]Sandia National Laboratories. Corresponding Author: msalle@sandia.gov
[2]Georgia Institute of Technology

Abstract:

Many systems can be approximated as linear with coefficients that vary periodically with time. For example, an anisotropic shaft rotating at constant speed on anisotropic bearings can be modeled as periodically time varying (PTV). Similar models can be obtained for wind turbines, some mechanisms, etc… However, the vast majority of modal analysis algorithms and techniques apply only to linear time invariant (LTI) systems. In this paper, two methods are demonstrated by which the free response of a periodically time varying system can be exactly parameterized by an LTI system. The parameters of the LTI representation can then be identified using standard techniques. The analysis techniques are demonstrated on a simple system, representing a rotor mounted on an anisotropic, flexible shaft, supported by anisotropic bearings. They are then applied to synthetic response data for a system with parameters that vary only weakly with time, as might be encountered when attempting to detect small cracks in a rotating shaft. These examples demonstrate the methods' ability to characterize the anisotropy of the shaft, even when both the shaft and supports are anisotropic.

1. Introduction

Periodically time varying (PTV) systems are encountered in many engineering fields. They were first studied as early as 1831 by well known figures such as Faraday, Rayleigh and Matheiu. More detailed studies were performed by Floquet and Lyapunov in the late 1800's, who independently studied linear differential equations with periodic coefficients [1], and arrived at similar results. Hence, the theory used to analyze such equations with is often called Floquet theory or Floquet-Lyapunov theory. Two well known periodically time varying differential equations are the Hill equation and the Mathieu equation. Richards [2] gave an excellent history of Floquet theory, and also reviewed a variety of applications, including: mass spectrometry, dynamic buckling of structures, elliptical waveguides, and electronics, focusing on second order systems. Montagnier, Spiteri and Angeles [3] give a good review of some recent research involving Floquet theory. These concepts have been applied to a variety of mechanical systems such as helicopters, wind turbines or other bladed machines [4], [5], mechanisms [3], buckling problems [4] and satellites. Recently, the methods have also been applied to create analytical models of rotordynamic systems [6], [7], [8], [9]. Sinha *et al* [10] and Montagnier et al [3] have applied Floquet theory to automatic control of periodically time varying systems.

While a number of powerful tools exist for modeling, controlling and assessing the stability of PTV systems, these are not always exploited in many applications where they could be of great advantage. Furthermore, there has been little work in developing methods for experimentally parameterizing PTV systems. While a wealth of tools, such as experimental modal analysis, exist for identifying the parameters of Linear Time Invariant (LTI) dynamic systems, most of these tools cannot be applied to linear PTV systems, so that one must use more difficult analysis methods. For example, there are well established methods for identifying the

parameters of LTI systems, and once the parameters of an LTI system have been identified, one can easily predict the response of the system to a variety of inputs. On the other hand, no comparable methods exist to experimentally characterize the behavior of time-varying systems, nor to efficient methods exist for computing their response to arbitrary inputs. In view of the similarities between linear periodically time varying systems and LTI systems, one might expect to be able to extend many of the tools for LTI systems to LPTV systems. This work demonstrates one such case in which system identification routines for LTI systems can be readily adapted to LPTV systems.

A number of methods have been proposed for treating systems whose parameters vary slowly with time. For example, those presented by Bendat and Piersol in [11]. In contrast, the methods presented here allow the treatment of systems whose parameters vary rapidly relative to the fundamental time constant of the system (i.e. the time constant of the system for a fixed set of parameters.) Particular attention is given to systems whose parameters vary only slightly with time. A rotordynamic system with a cracked or slightly anisotropic shaft in anisotropic bearings typifies such a system.

The following section reviews some aspects of Floquet-Lyapunov theory for periodically time varying ordinary differential equations and presents two strategies for identifying the parameters of PTV systems from free response data. In Section 3 these methods are applied to synthetic data for two PTV systems, one in which the system parameters vary strongly with time, and another with only slight variation as might be encountered in condition monitoring applications. Section 4 presents some conclusions.

2. Theoretical Development

2.1. Review of Floquet-Lyapunov Theory for PTV Systems

This section presents a brief review of the relevant aspects of Floquet Theory, as well as some justification using concepts from discrete system theory. The equations governing a linear time varying system may be written in the following state space representation

$$\dot{x} = A(t)x + B(t)u \qquad (1)$$

where x is the system state vector, $\{u\}$ the inputs to the system, and the matrices $A(t)$ and $B(t)$ vary with time. If the input $u\} = 0$, then the state transition matrix can be used to transfer the state vector from the initial state $x(t_0)$ at time t_0 to the state at time t as follows

$$x(t) = \Phi(t, t_0)x(t_0) \qquad (2)$$

with the property that

$$\Phi(t, t_0) = \Phi(t, t_1)\Phi(t_1, t_0)\,. \qquad (3)$$

If the dynamics of the system from time t_0+T_A to $t+T_A$ are the same as those from time t_0 to t, so that $A(t)$ is periodic with period T_A, then the state transition matrix for $t \geq 0$ can be reconstructed from the state transition matrix for $0 \leq t < T_A$ as follows [3]

$$\Phi(t + nT_A, t_0) = \Phi(t, t_0)\Phi(t_0 + T_A, t_0)^n \qquad (4)$$

where n is an integer. This important result is often exploited to efficiently compute the response of linear periodically time varying systems [4]. A few methods for computing the state transition matrix are discussed in the Appendix.

The Floquet-Lyapunov theorem states that the state transition matrix of a linear PTV system with period T_A can be decomposed as follows [4]

$$\Phi(t, t_0) = P(t)^{-1} \exp\big(R(t - t_0)\big)P(t_0)\,, \qquad (5)$$

where R is a constant matrix and $P(t)$ is periodic such that $P(t+T_A)=P(t)$. Both matrices can be complex in general [3]. If R can be diagonalized as

$$R = (M_R)\Lambda_R(M_R)^{-1} \qquad (6),$$

then the Floquet-Lyapunov representation can be expressed in terms of modal parameters with time varying mode shapes $\{\psi_r\}$ as follows

$$\Phi(t,t_0) = P(t)^{-1} M_R \exp\left(\Lambda_R (t-t_0)\right) M_R{}^{-1} P(t_0)$$
$$\Phi(t,t_0) = \Psi(t) \exp\left(\Lambda_R (t-t_0)\right) \Psi(t_0)^{-1} \ , \ \Psi(t) = P(t)^{-1} M_R \qquad (7),$$

where $\Psi(t)=[\{\psi_1\}, \{\psi_2\}, \ldots]$ is the time varying modal matrix and Λ_R contains the constant Floquet eigenvalues of the system.

2.2. Identifying the parameters of PTV systems

In this section we shall present two methods by which the free response of a periodically time varying system can be represented exactly by that of an LTI system. The first method consists of discretizing the PTV system over its fundamental period, resulting into a collection of LTI systems of the same order as the PTV system, corresponding to different portions of the fundamental period. The second method expands the modal matrix of the Floquet representation in a Fourier series, resulting in a single, although possibly high order, LTI representation for the PTV system. In either case, the parameters of the LTI system (or collection of systems) can be identified from the transformed response using standard system identification techniques. The parameters identified for the LTI system are then easily related to those of the PTV system. The relative merits of these two methods will be discussed throughout the remainder of the paper.

2.2.1. Method #1

From the state transition matrix representation in eq. (4), one can construct a discrete time system whose response exactly matches that of the LPTV system at the instants $t_0 + nT_A$ where n is an integer. First define $x(n) = x(nT_A+t_0)$ where $n = 0, 1, 2, \ldots$ Then one can see that

$$x(n+1) = \Phi(t_0 + T_A, t_0) x(n) = A_D(t_0) x(n) \qquad (8),$$

where the matrix $A_D(t_0)$ is constant for a given initial time t_0. This shows that the samples at instants separated by integer multiples of T_A are related by a linear time invariant system whose parameters depend only on the initial time t_0. As a result, one can identify the parameters of the matrix $A_D(t_0)$ using standard methods for LTI systems, so long as the samples are taken at instants separated by integer multiples of T_A.

This method requires that one sample synchronous with T_A. However, it might be desirable to sample the response at a higher or lower rate. This can be achieved by setting the time increment $\Delta t = T_A/P$ or $\Delta t = P*T_A$, where P is an integer. Setting $\Delta t = P*T_A$ corresponds to sampling once every P periods of the system. The system matrix identified from such a response would then be $(A_D)^P$. (One might also interpolate the response data if Δt is selected arbitrarily, but doing so may introduce interpolation error.)

The more interesting situation occurs when one samples at a faster rate (such that $\Delta t = T_A/P$). In this case one can learn something about the time varying nature of $A(t)$. In this case, the response is separated into the following collection of responses.

$$y_0 = [t_0, t_0 + T_A, t_0 + 2T_A, \cdots, t_0 + N_c T_A]$$
$$y_1 = [t_1, t_1 + T_A, t_1 + 2T_A, \cdots, t_1 + N_c T_A]$$
$$\cdots \qquad (9),$$
$$y_{P-1} = [t_{P-1}, t_{P-1} + T_A, t_{P-1} + 2T_A, \cdots, t_{P-1} + N_c T_A]$$

Each response y_K can be parameterized by a matrix $(A_D)_k$, pertaining to a different initial time t_k where $t_k = k*T_A/P$ for k = 0,1,…P-1. The system parameters can then be determined by applying a standard, LTI modal parameter identification routine to each response y_k independently. In the time domain, for example, one might use the Least Squares Complex Exponential method or a Subspace method [12, 13]. If the responses are transferred to the frequency domain, the Least Squares Complex Frequency Domain Algorithm (LSCF) [14] or the Algorithm of Mode Isolation (AMI) [15-18] could be used.

Some of the aforementioned algorithms estimate the system matrix $(A_D)_k$ directly whereas others identify the modal parameters that comprise it. The modal parameters are related to the system matrix as follows

$$A_D(t_k) = (A_D)_k = M_k \Lambda_k M_k^{-1} \qquad (10),$$

where M_k is the modal matrix whose columns contain the state space mode vectors and Λ_k is a diagonal matrix of eigenvalues.

Comparing equation (10) with equation (7) and recalling that A_D is a state transition matrix, one can see that when the Floquet state transition matrix in eq. (7) is diagonalizable, the eigenvalues of each matrix $(A_D)_k$ should be equal (i.e. $\Lambda_k = \Lambda = exp(\Lambda_R T_A)$ for all k) and their respective mode vectors should be the periodic Floquet mode vectors $\{\psi(t_k)\}$. In such a case, one can readily relate the modal parameters of the systems $(A_D)_k$ to the Floquet-Lyapunov representation. This was found to be the case for the PTV system presented herein using a variety of different parameter sets.

When the eigenvalues Λ_k of $(A_D)_k$ are not a function of k, the modal parameters of the systems $(A_D)_k$ can be found in a single pass using a "common denominator" parameter identification algorithm. The set of responses $\{y_k\}$ are processed as if they resulted from a single SIMO experiment with N_o*P outputs. This results in a global estimate of the eigenvalues, and an estimate of the mode shapes for each system $(A_D)_k$. For some systems this treatment might entail processing data from a large number of outputs simultaneously, in which case the authors recommend using either the AMI or the LSCF algorithms.

At this juncture it is important to note that the imaginary parts of the eigenvalues of the matrices $(A_D)_k$, even when constant with k, can differ from the Floquet eigenvalues by an integer multiple of the fundamental frequency of the parameters of the PTV system $\omega_A = 2\pi/T_A$. This aliasing phenomenon is a well known feature of Floquet-Lyapunov theory [4]. Moreover, it is reasonable considering that the matrices $(A_D)_k$ are only related to the system response at the instants $t_k + nT_A$. However, if one considers the response at all time instants (i.e. for $[t_0, t_1, \ldots, t_P, t_{P+1}]$), one can usually determine the integer multiple that relates the aliased eigenvalues to the true Floquet eigenvalues, as will be elaborated in the following sections.

2.2.2. Method #2

The Floquet representation of the response in eq. (7) can be expressed in summation form as follows

$$\Phi(t,t_0) = \sum_{r=1}^{2N} (A_R)_r \exp(\lambda_r (t - t_0))$$
$$(A_R)_r = \{\psi_r(t)\}\langle L_r(t_0)\rangle \qquad (11),$$

where N denotes the number of modes, $\psi_r(t)$ are the mode vectors or the columns of $[\Psi(t)]$, and $L_r(t)$ are the modal participation factors, or the rows of $[\Psi(t)]^{-1}$. The residue matrices $(A_R)_r$ are the product of a periodic column vector and a periodic row vector, and hence are themselves periodic. Because they are periodic, they can be readily expanded in a Fourier series. Here we shall assume that they can be accurately represented using a fixed number $(2*N_R + 1)$ of terms so that the response may be written as

$$\Phi(t,t_0) = \sum_{r=1}^{2N} \left(\sum_{m=-N_R}^{N_R} [B]_{r,m} \exp(im\omega_A (t - t_0)) \right) \exp(\lambda_r (t - t_0)) \qquad (12),$$

where $[B]_{r,m}$ is the mth complex Fourier coefficient of the rth residue matrix and $\omega_A = 2\pi/T_A$. Factoring out the summations reveals the nature of the response.

$$\Phi(t,t_0) = \sum_{r=1}^{2N} \sum_{m=-N_R}^{N_R} [B]_{r,m} \exp((\lambda_r + im\omega_A)(t - t_0)) \qquad (13)$$

This can be thought of as the impulse response of an LTI system with $2*N*(2*N_R + 1)$ eigenvalues $\lambda_r + i*m*\omega_A$. The amplitude of each mode's response is determined by the magnitude of the Fourier coefficient of its residue matrix. The response and hence the state transition matrix must be real, so one can see that every complex eigenvalue must be

accompanied by it's complex conjugate and that the Fourier coefficients of the residue matrices must also be real or part of a complex conjugate pair.

The response in eq. (13) is indistinguishable from the response of a state-space LTI system having eigenvalues $\lambda_r + i*m*\omega_A$. Hence, one can identify the parameters in eq. (13) from the time response or FFT of the time response directly using any standard parameter identification algorithm for LTI systems. Equation (13) can then be used to interpret the result and/or reconstruct the Floquet representation.

2.2.3. Comparison and Discussion

One important difference between the identification methods is that Method #1 requires that the system response be sampled synchronous with the shaft angle or at a high enough rate that the response can be interpolated to a fixed set of shaft angles, whereas Method #2 places no special restriction on the sample rate. (A variety of data acquisition systems are capable of sampling in such a manner.) Another important distinction between the methods is that in general a much lower order system will be identified using Method #1, although it may have many outputs. For Method #2, the system order, which depends on the number of terms in the Fourier series expansion of the residues, can be expected to be higher. Each term required in the expansion increases the number of poles to be identified from the response. For many Experimental Modal Analysis (EMA) algorithms, the complexity of the identification process is governed by the number of poles in the response. On the other hand, a large number of response data sets are readily accommodated.

When Method #1 is employed, standard EMA algorithms can identify the Floquet eigenvalues of the system utilizing all data simultaneously. This is often called global curve fitting in the EMA literature. On the other hand, to globally estimate the Floquet eigenvalues using Method #2, one must add a constraint in the fitting process to assure that the imaginary parts of each Floquet eigenvalue occur at integer multiples of $\omega_A = 2\pi/T_A$ (which is known). If the eigenvalue and each of its multiples is estimated independently, one will likely end up with various estimates of the Floquet eigenvalue, each of which is likely to be somewhat different. This process could be greatly complicated if the system has many eigenvalues, especially if any of the contributions at $\lambda_r + i*m*\omega_A$ overlap for any eigenvalue λ_r and any m corresponding to a significant Fourier coefficient $[B]_{r,m}$.

When Method #1 is used, one must "un-alias" the identified eigenvalues by determining the integer multiple of the fundamental frequency of the system parameters relating each to its corresponding Floquet eigenvalue. This might be difficult when dealing with a high order system. In general, the best practice is probably to combine the information derived from each of the two approaches.

3. Identification Examples

In order to present the basic modeling and identification concepts as clearly as possible, a very simple LPTV system will be considered. The system consists of a modified Jeffcott rotor on an anisotropic shaft that is supported by anisotropic bearings. The system dynamics are equivalent to those of the discrete system in Figure 1. The discrete system consists of a point mass suspended by two orthogonal, massless springs with spring constants k_{Rx} and k_{Ry}. The springs are attached to a massless turntable that turns at constant speed Ω. The turntable is fixed to ground by two massless springs k_{Fx} and k_{Fy}. The equations of motion for this system are given in the Appendix. Proportional damping is added to the system via the factor c_f (see Section 5.2 in the Appendix.) For the first example, the springs representing the shaft stiffness are significantly different, resulting in a system whose stiffness matrix is a strong function of time. The second example illustrates the system identification techniques described previously on noise contaminated data for a system with parameters that vary weakly with time. This is analogous to detecting a crack in the shaft in the presence of measurement noise.

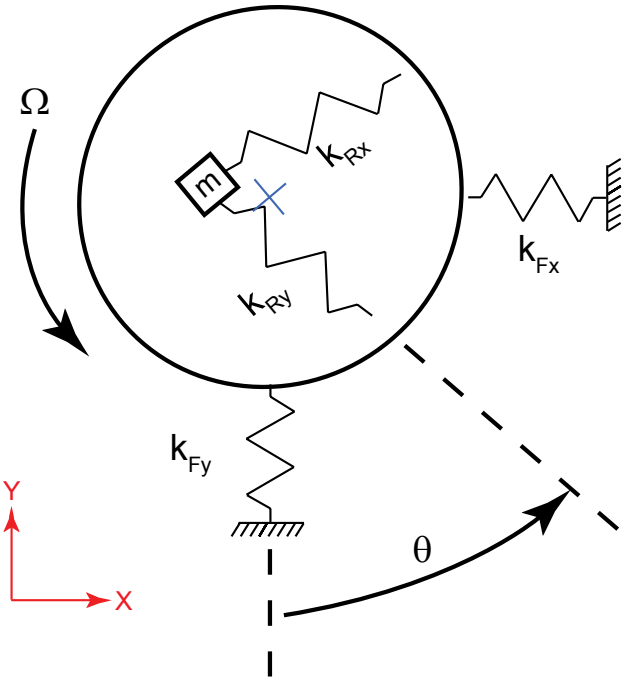

Figure 1: Schematic of Simple PTV System

3.1. Strongly PTV Example

The following parameters are used for this example. (See section 5.2 in the Appendix for the equations of motion.)

$k_{Rx} = 1$ $k_{Ry} = 1.2$ $c_f = 0.004$	$k_{Fx} = 1$ $k_{Fy} = 1.5$	$m = 1$ $\Omega = 0.5$

With these parameters, the fixed shaft natural frequencies of the system varied between 0.707 and 0.911 rad/s depending on the angle at which the shaft was fixed.

The response of the system to a unit impulse is identical to the free response of the system to a unit initial velocity (scaled by the mass, unity in this case) in the direction of the force. (This can be seen by integrating the equations of motion from 0^- to 0^+.) A unit initial velocity at an angle of 45 degrees was used to assure that both modes of the system were excited, which corresponds to taking the initial state vector to be $x_0 = [0, 0, 0.707, 0.707]^T$. The equations of motion are periodic with a period $T_A = 6.2832 = 2\pi$, which corresponds to one half of a revolution of the shaft. The sample increment was chosen to be $\Delta t = 0.12566$, corresponding to 50 samples per half revolution of the shaft. The impulse response was found using time integration, via Matlab's "ode45" function. (This result was compared with that obtained by approximating the system matrix as piecewise constant over 50 increments, as discussed in Section 5.1 of the Appendix. The two responses were almost indistinguishable.) The response was evaluated over a time window encompassing 512 revolutions of the shaft, which was adequate to allow the impulse response to decay to a small fraction of its initial amplitude.

3.1.1. Method #2 - Strongly PTV System

The Fast Fourier Transform of the full record of the impulse response of this time varying system is shown in Figure 2. The displacement in the fixed reference frame in both the *x* and *y* directions is shown. A number of peaks are evident in the FFT, even though the system has only two natural frequencies. The presence of additional peaks is explained by eq. (13), which states that the free response will have harmonic components at the damped natural frequencies $imag(\lambda_r)$, and at the damped natural frequencies plus or minus integer multiples of the fundamental frequency of the system parameters ω_A. For this system, one might expect the

Fourier series coefficient corresponding to m = 0 in eq. (12) to dominate the response. In that case, one can deduce that the Floquet natural frequencies are located near 0.8 rad/s where the two dominant peaks occur. The other peaks must then correspond to contributions at $\lambda_r + i*m*\omega_A$ for m = 2 and at $(-\lambda_r + i*m*\omega_A)$ for m = 1 and 2. (Note that $\omega_A = 2*\pi/T_A = 1$ in this example.) One could use a curve fitting routine to determine the frequencies more precisely, or to determine the coefficients $[B]_{r,m}$ and assemble the Floquet representation.

If one did not know which Fourier series coefficient was dominant in the expansion in eq. (12), then there might be some ambiguity in determining the Floquet eigenvalues and assigning the terms of the Fourier series to the proper indices (*m*).

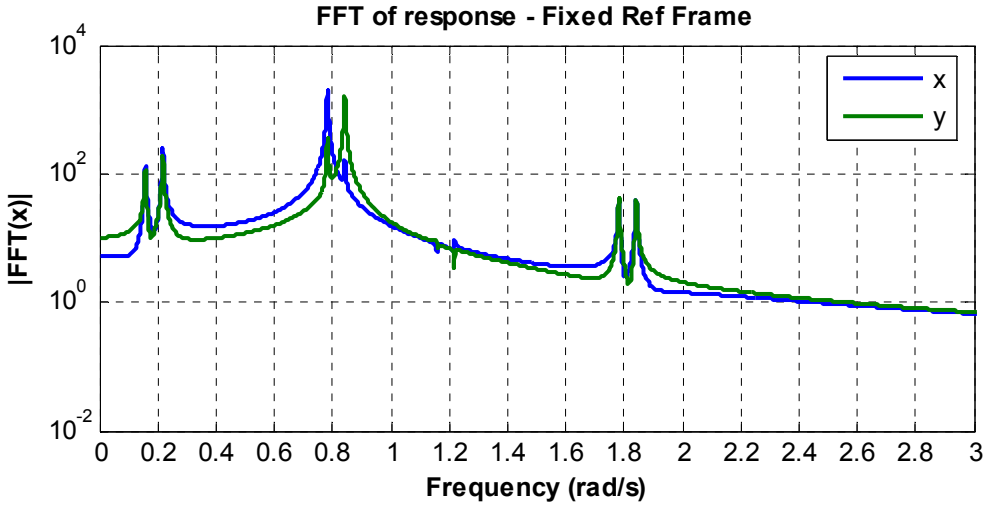

Figure 2: FFT of impulse response of 2nd order strongly PTV system. (FFT of entire impulse response.)

3.1.2. Method #1 - Strongly PTV System

Method #1 gives quite a different view of the same data. Figure 3 shows the FFT of the same data after decomposing it into a set of *P = 50* LTI systems as discussed in Section 2.2.1. (Each LTI response corresponds to samples spaced T_A seconds apart in time, beginning at $t_k = k\Delta t$ for *k = 0, 1 … P*, as was described in Section 2.2.1.) Each of these responses can be described by an LTI system. Response contributions are only visible at two frequencies, as one would expect for a 2-DOF system. The peaks in the FRF appear at about 0.17 and 0.22 rad/s. These must be the Floquet eigenvalues, plus or minus some factor of the fundamental period of the system parameters ω_A.

If these results are combined with the information in Figure 2, one can deduce that these peaks correspond to $\omega_A - imag(\lambda_r)$ where $imag(\lambda_r)$ is the primary frequency component observed in Figure 3. Hence, the first and second peaks observed here correspond to the second and first of the peaks observed near 0.8 rad/s in Figure 2. This difference in frequencies can be attributed to aliasing, as described previously.

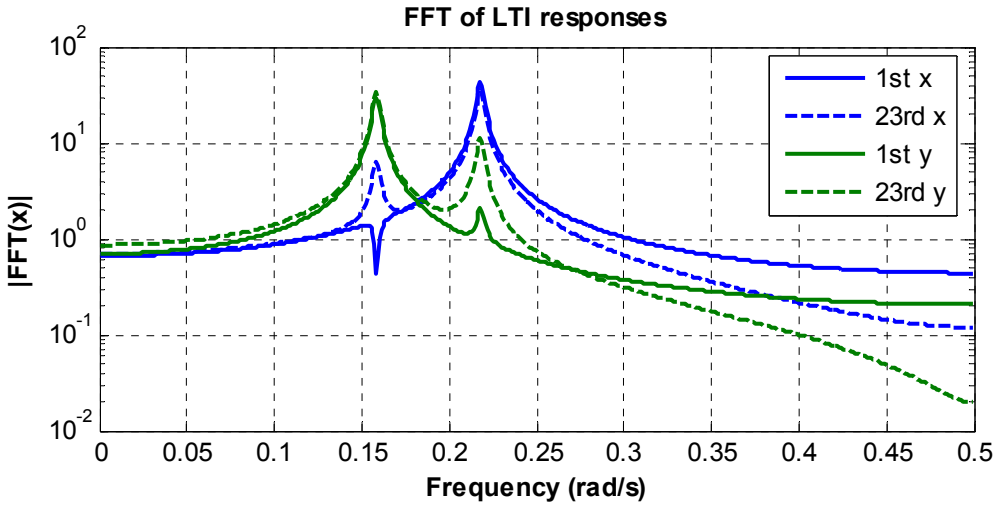

Figure 3: FFT of LTI responses, found by decomposing the impulse response in Figure 2 into that of a collection of 50 LTI systems. Responses for k = 0 and 22, corresponding to starting times t_0 = 0 and 2.7646 are shown.

The modal parameters of this collection of LTI systems can be extracted using any SIMO modal parameter identification algorithm. The Algorithm of Mode Isolation [15-18] was applied to the collection of LTI responses in order to determine the eigenvalues and residue vectors of the modes comprising the response. AMI processed a total of 100 FRFs simultaneously, 50 responses in the x direction and 50 in the y direction. The algorithm extracted the parameters automatically as described in [18]. The natural frequencies identified by AMI were 0.1582 and 0.2178, which were within a fraction of a percent of the analytical values, computed from the State Transition Matrix. The modal damping ratios identified by AMI were 1.29 and 0.938 percent, which were within 1% of the analytical values.

The residues identified are shown in Figure 4, the top and bottom panes displaying the residues in the x- and y- directions respectively. These residues were normalized as described in the Appendix (designated A_{zero}) so as to be proportional to the time varying Floquet mode vectors. The variation in the residues with shaft angle is clearly apparent. The identified residues overlay the analytically derived residues.

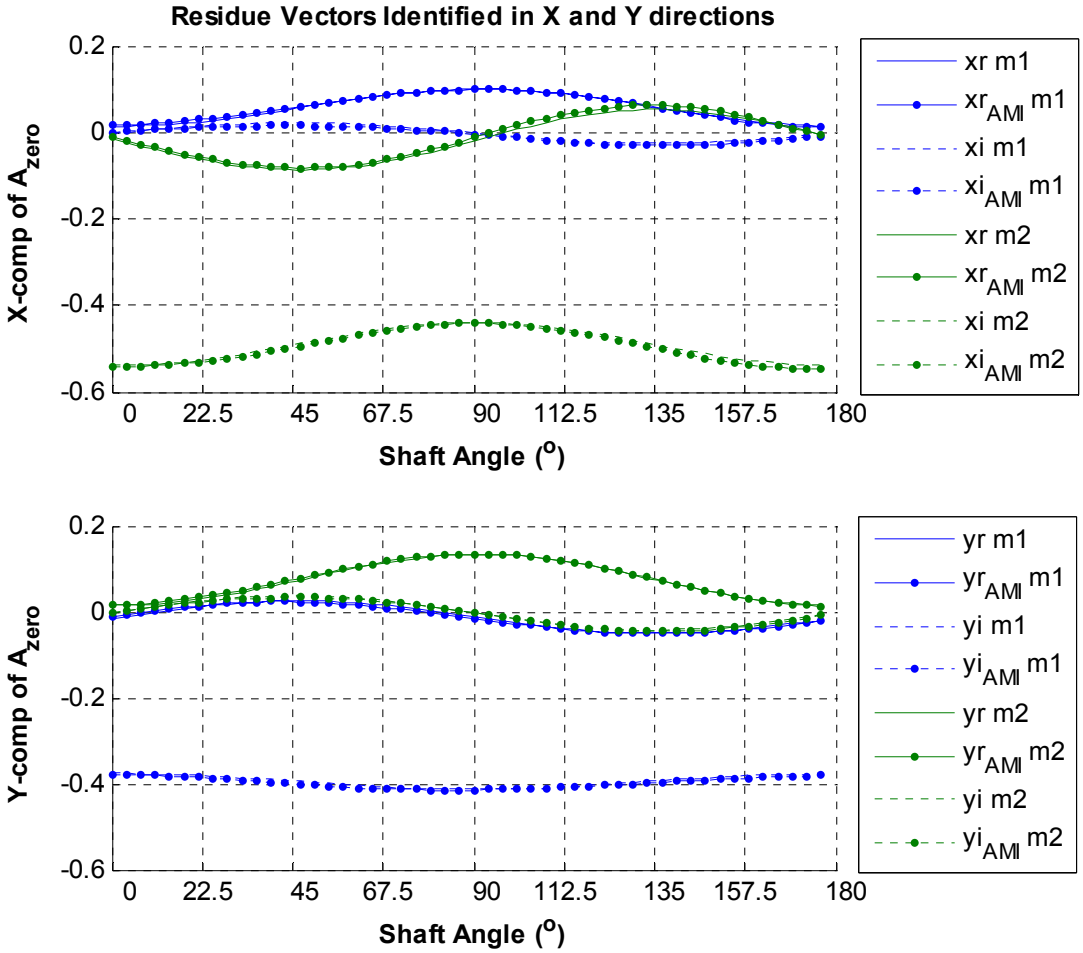

Figure 4: Real ('r') and Imaginary ('i') components of modal residues identified by AMI from the data decomposed into LTI responses (Method #1: Two of the LTI responses that were curve fit are shown in Figure 3.) The analytically derived residues are also shown, which overlay the identified ones.

3.1.3. Discussion

This example illustrates a few important features of PTV systems. The example system is 2nd order with time varying mode shapes. When the response is decomposed according to Method #1, only two resonant peaks, corresponding to two distinct eigenvalues, appear in the response. However, the mode shapes identified by this method vary with shaft angle. On the other hand, if the entire time response of the PTV system is considered as in Figure 2, a number of peaks are seen in the response spectrum, each corresponding to a Floquet natural frequency plus some integer multiple of the shaft speed. The residues identified for each of the modes corresponding to a single Floquet eigenvalue (i.e. $\lambda_r + i*m*\omega_A$) must be collected to assemble the Fourier series expansion of the time varying residue.

Visual inspection of Figure 4 suggests that the zero frequency term should be dominant in a Fourier series expansion of residues. It also appears than any term in the expansion beyond m = 2 or 3 would be small relative to the first few terms. These observations confirm the validity of the qualitative results derived using Method #2. Taken together, the two methods provide adequate information to attain a valid characterization of the system.

3.2. Weakly PTV Example (Cracked Shaft)

One problem of interest is that of detecting cracks in a shaft that is supported in anisotropic bearings. A crack in a round shaft is likely to cause the bending moment of inertia of the shaft to be different in two orthogonal directions. The anisotropy of both the shaft and the bearings cannot both be captured by an LTI model. However, the system fits a Floquet representation very well.

The parameters of the simple PTV system were modified to simulate a shaft with a small level of anisotropy in anisotropic bearings. The same parameters used previously were used in the model with the exception of the stiffness parameters for the shaft k_{Rx} and k_{Ry}. These were set at k_{Rx} = 1 and k_{Ry} = 1.05, corresponding to a difference in stiffness of only 5%. The Floquet mode shapes for the system are displayed in Figure 5. The mode shapes are almost constant with shaft angle, as one might expect for a system that is almost isotropic.

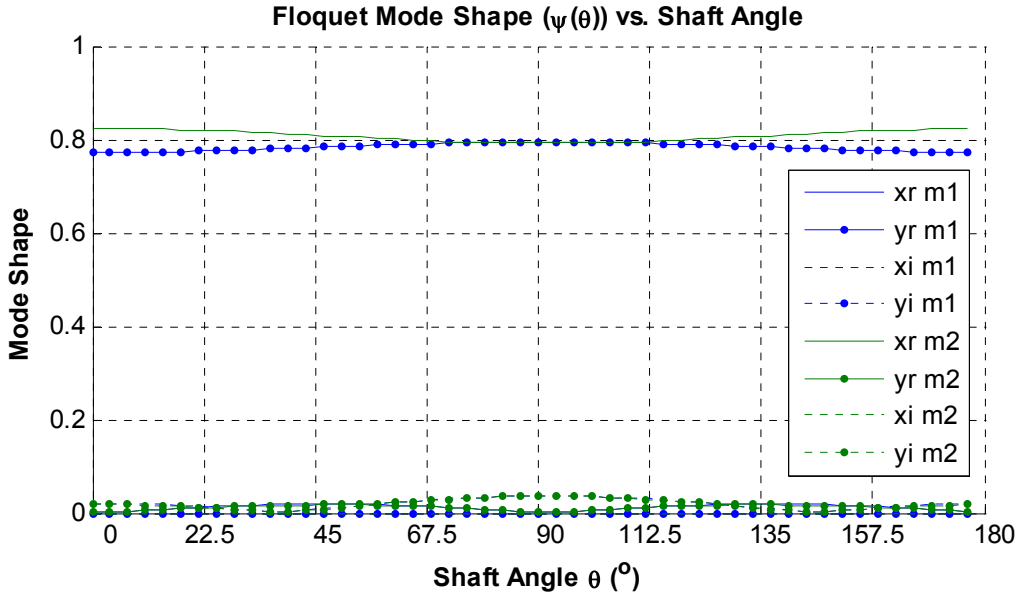

Figure 5: Floquet Mode shapes in the x- and y- directions versus shaft angle for the cracked shaft system. 'r' and 'I' denote the real and imaginary parts of the mode coefficients respectively.

The response of this system was simulated as was done previously for the strongly PTV system. Gaussian white noise, scaled to have a standard deviation equal to 5% of the maximum of each impulse response was then added to the impulse responses to investigate the robustness of the identification methods to noise. Figures 6 and 7 show the noise contaminated response of the data for the periodically time varying system. Figure 6 shows the FFT of the PTV response (Method #2), while Figure 7 shows the FFT of the same data decomposed via Method #1.

Only two frequency components are prominent above the noise in the response in Figure 6. These frequency components correspond to the two Floquet eigenvalues. One must inspect the data carefully to detect the contributions at $-\lambda_r + i*m*\omega_A$ for m = 1 and 2. The contribution at $\lambda_r + i*1*\omega_A$ is not visible above the noise. Consequently, careful treatment of the data is required to detect the periodically time varying nature of the system, yet it can be detected if one knows what features to look for.

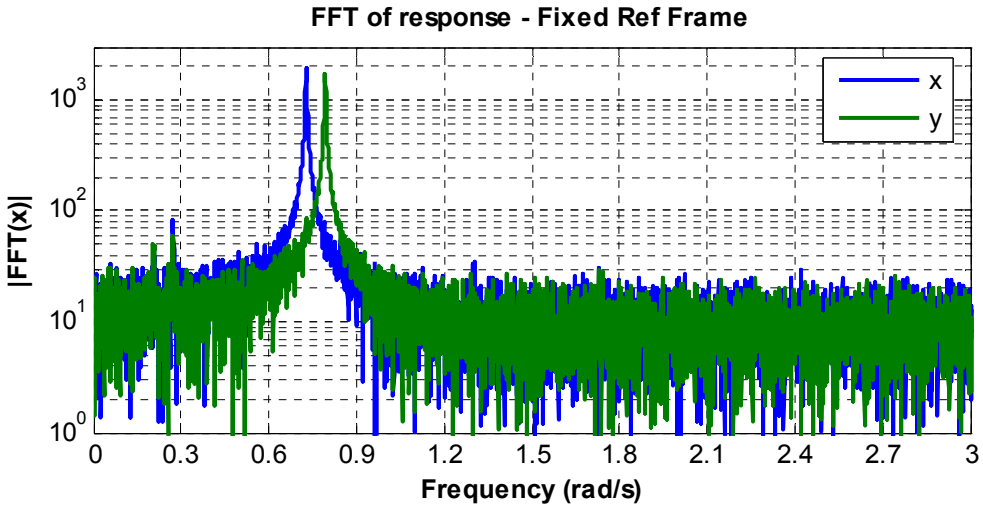

Figure 6: FFT of noise contaminated impulse response of 2nd order weakly PTV system. (FFT of entire impulse response.)

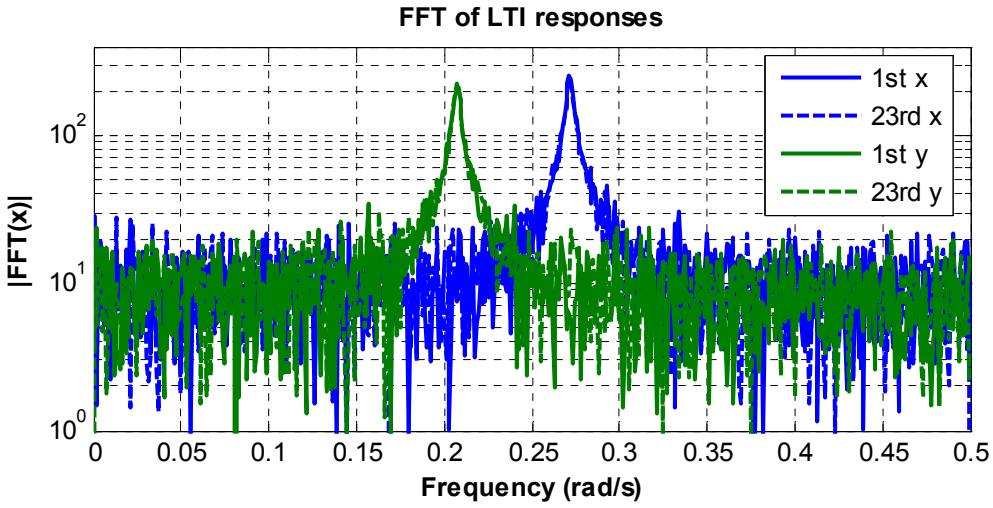

Figure 7: FFT of LTI responses found by decomposing the impulse response in Figure 6 into 50 separate responses, each of which has LTI dynamics. Responses for k = 0 and 22, corresponding to starting times t_0 = 0 and 2.7646 are shown.

The Algorithm of Mode Isolation [15-18] was applied to the collection of LTI responses in Figure 7 in order to determine the eigenvalues and residue vectors of the modes comprising the response. A composite FRF, created by averaging the magnitude of all 100 FRFs, is shown in Figure 8, along with a composite of AMI's reconstruction of the data. A composite of the difference between the two is also shown. The response fits the data well, the difference being at the noise level.

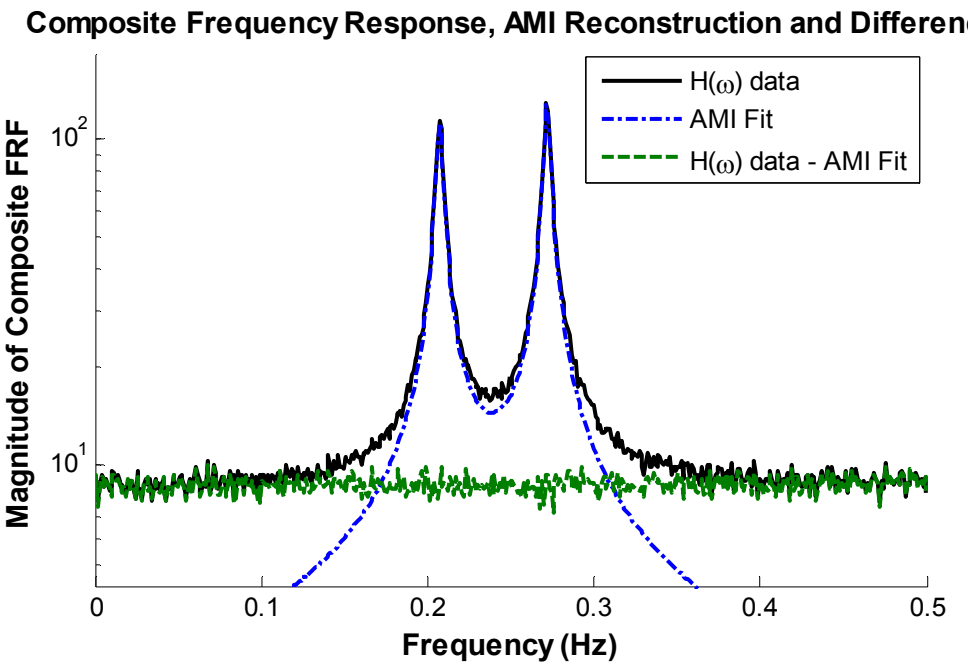

Figure 8: Composite FRF of the LTI data comprising 100 FRFs, AMI's reconstruction and the difference.

The modal residues extracted by AMI were brought to a common reference using the procedure in the Section 5.3 of the Appendix. These are shown in Figure 9. (The shifting discussed in the Appendix requires knowledge of the Floquet eigenvalues, which were found by shifting the eigenvalues identified by AMI by the (known) fundamental frequency of the system parameters ω_A.)

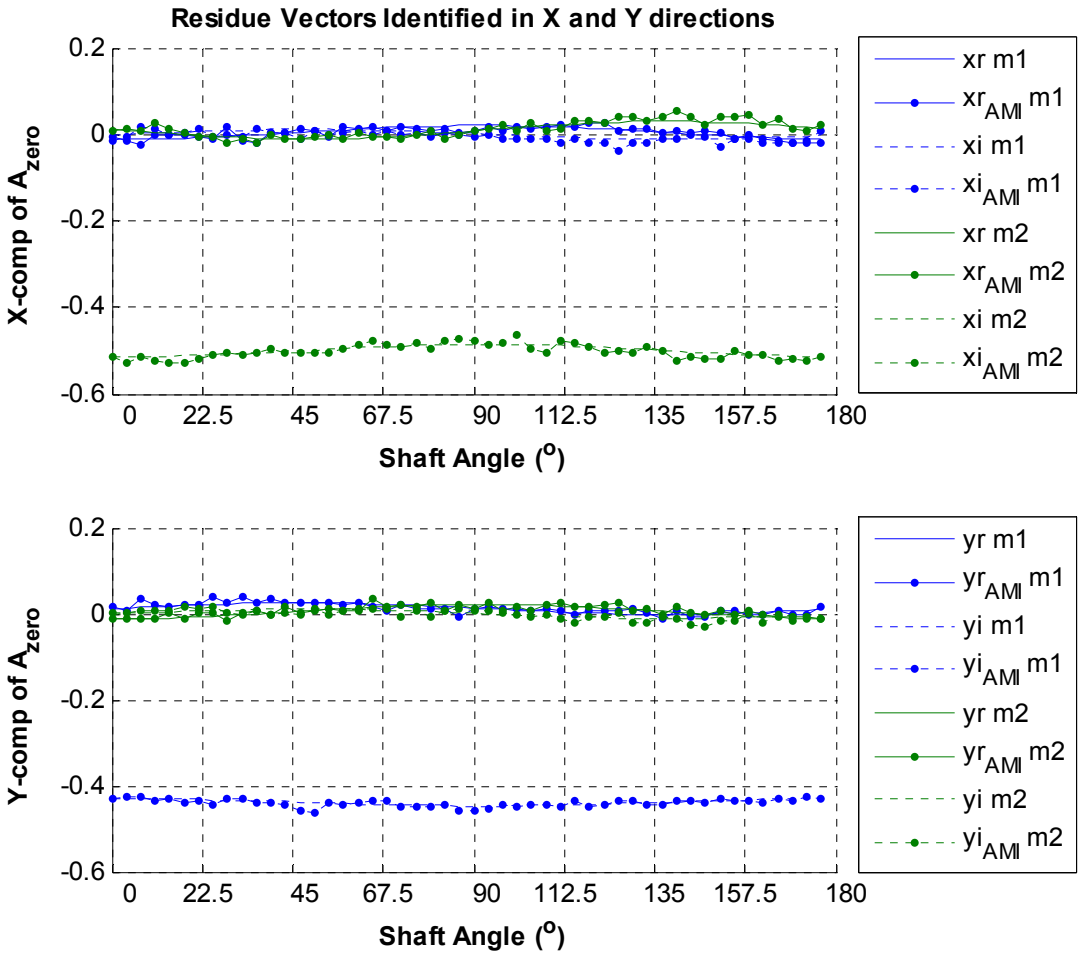

Figure 9: Modal residues identified by AMI from the noise contaminated response data, compared with the analytically derived residues.

The modal residues in Figure 9 appear to be essentially constant with shaft angle. Figure 10 plots the imaginary parts of the residues after subtracting their mean values to enhance the visibility of the variation with shaft angle. The residue vectors agree fairly well with the analytical ones, although the variation with shaft angle stands out only slightly above the noise.

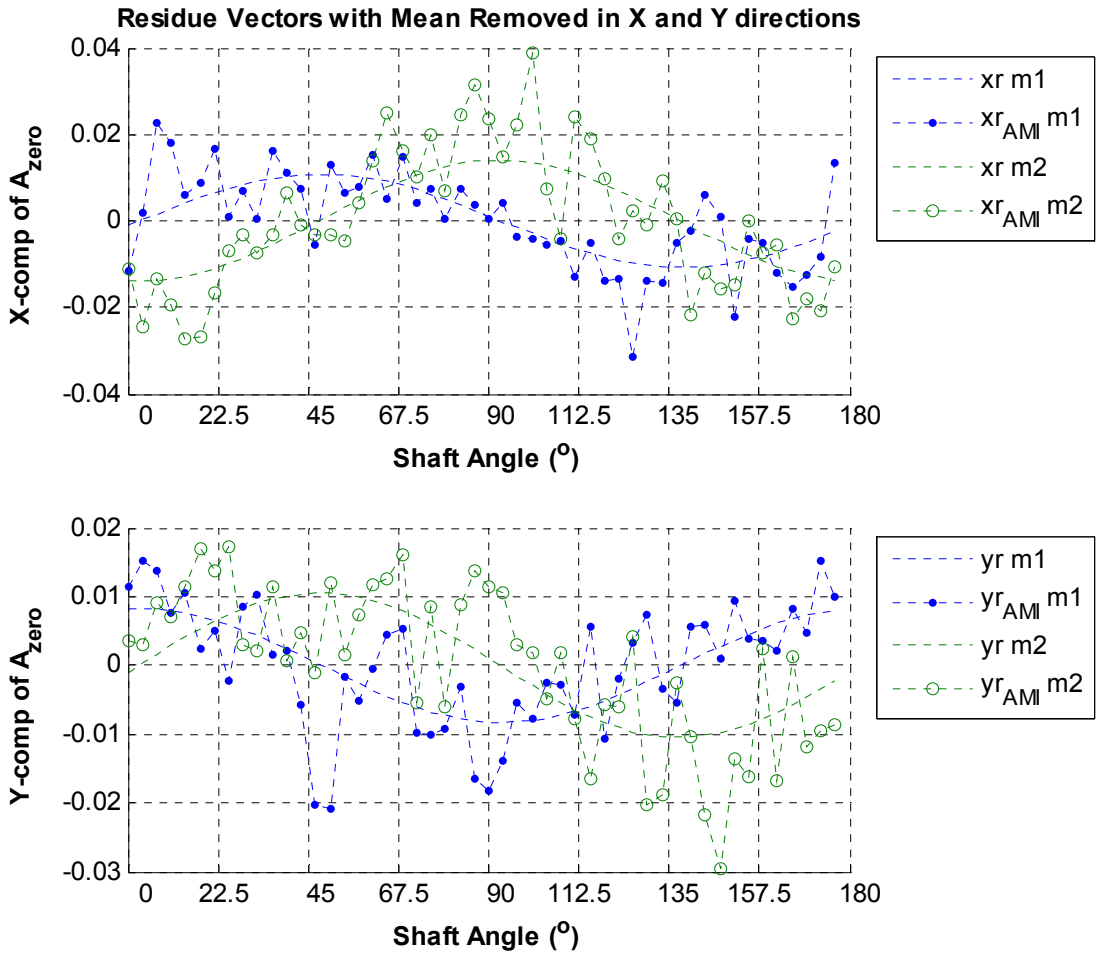

Figure 10: Imaginary parts of residues identified by AMI with the mean removed to accentuate their variation with shaft angle.

4. Conclusions

The preceding examples have demonstrated that the parameters of linear, periodically time varying systems can be identified from the system's free response (or impulse response) using conventional tools for linear time invariant systems. Two methods have been investigated. The first breaks the response of the periodically time varying system into that of a number of low-order LTI systems, the collection of which can be treated using standard methods for LTI systems. The second method deals with the response of the periodically time varying system directly, using its Fourier series expansion to explain all of the frequency content observed in the response. Standard system identification techniques can also be applied when using this second method, although a rigorous, global treatment of the data requires more specialized techniques, which can apply a constraint to the identified eigenvalues. Either method can be used to detect a weak time-variation in the system parameters, even in the presence of noise. For the simple low order system studied here, both methods appear to be of approximately equal value. The first method may provide some advantage in future work, when higher order systems are studied.

5. Appendix

5.1. Computing the State Transition Matrix

Considering the importance of the state transition matrix to the development here, some comments regarding how the state transition matrix can be computed are in order. First we recall that the state transition matrix need only be computed for one period or for $0<t<T_A$. The most common approach is to use a time integration method such as Runge-Kutta (i.e. "ode45.m" in Matlab). The state vector due to a unit initial condition in the first generalized coordinate $x(t_0) = [1, 0, 0\ldots0]^T$ is computed and the result is stored as the first column of $\Phi(t,t_0)$. This process is then repeated for the second generalized coordinate until all of the columns of $\Phi(t,t_0)$ have been populated. While this approach is conceptually simple, it is not very efficient. For example, Friedmann *et al* present a simple fourth order Runge-Kutta algorithm that solves for all columns of the state transition matrix simultaneously [4].

Another conceptually simple approach involves discretizing the domain $0<t<T_A$ into a number of subdomains $t_k<t<t_{k+1}$ over which the system matrix $A(t_k)$ is effectively constant. The state transition matrix from t_k to t_{k+1} can then be computed using the relationship for a linear system

$$\Phi(t_{k+1},t_k) = \exp\big(A(t_k)(t_{k+1}-t_k)\big) = M\exp\big(\Lambda(t_{k+1}-t_k)\big)M^{-1} \qquad (14),$$

where $A(t_k) = M\Lambda M^{-1}$ is the modal decomposition of $A(t_k)$. If the matrix $A(t_k)$ can be diagonalized, then the matrix exponential on the right can be computed as the diagonal matrix whose elements are the exponential of the diagonal elements of $\Lambda(t_{k+1}-t_k)$. If it cannot be diagonalized then one must use a different approach to compute the matrix exponential, such as the algorithm implemented in the 'expm' command in Matlab.

Once the matrices $\Phi(t_{k+1},t_k) = (A_S)_k$ have been computed, then the state transition matrices for the period starting at any initial time t_k can be easily computed as follows

$$\begin{aligned}\Phi(T_A,t_0) &= (A_S)_{Ns-1}(A_S)_{Ns-2}\cdots(A_S)_0 \\ \Phi(t_k+T_A,t_k) &= (A_S)_{k-1}(A_S)_{k-2}\cdots(A_S)_0(A_S)_{Ns-1}(A_S)_{Ns-2}\cdots(A_S)_k\end{aligned} \qquad (15)$$

where Ns is the number of time steps used to discretize the domain $0<t<T_A$.

A multitude of other algorithms exist. Montagnier *et al* [3] present an algorithm that solves a boundary value problem to obtain the state transition matrix. Sinha and his associates presented an algorithm that uses Chebyshev polynomials to compute a symbolic approximation of the state transition matrix [19, 20].

5.2. Equations of Motion for Simple PTV System

The equations of motion follow where the state vector contains the response in the *x* and *y* directions in the fixed reference frame.

$$\begin{aligned}&[M]\begin{Bmatrix}\ddot{X}\\ \ddot{Y}\end{Bmatrix} + [C]\begin{Bmatrix}\dot{X}\\ \dot{Y}\end{Bmatrix} + [K_{PTV}]\begin{Bmatrix}X\\ Y\end{Bmatrix} = \begin{Bmatrix}0\\ 0\end{Bmatrix} \\ &[M] = \begin{bmatrix}m & \\ & m\end{bmatrix},\ [C] = c_f[K_F] \\ &[K_{PTV}] = \Big([R][K_R][R]^T - [R][K_R][R]^T\big([R][K_R][R]^T + [K_F]\big)^{-1}[R][K_R][R]^T\Big) \\ &[K_R] = \begin{bmatrix}k_{Rx} & \\ & k_{Ry}\end{bmatrix},\ [K_F] = \begin{bmatrix}k_{Fx} & \\ & k_{Fy}\end{bmatrix},\ [R] = \begin{bmatrix}\cos(\Omega t) & \sin(\Omega t)\\ -\sin(\Omega t) & \cos(\Omega t)\end{bmatrix}\end{aligned} \qquad (16)$$

Note that a damping matrix is included which is set proportional to the turntable stiffness matrix.

5.3. Relating Residue Vectors to Mode Vectors

It is important to note that although that the residues identified from the collection of LTI systems used in Method #1 are proportional to the mode vectors when taken individually, the constant of proportionality for each residue is different. In Figures 4 and 9, the residues have been rescaled so that the constant of proportionality is not a function of shaft angle. The method for rescaling the residues will be explained in this section. Figure 11 shows the residue vectors identified by AMI for the strongly PTV system before rescaling.

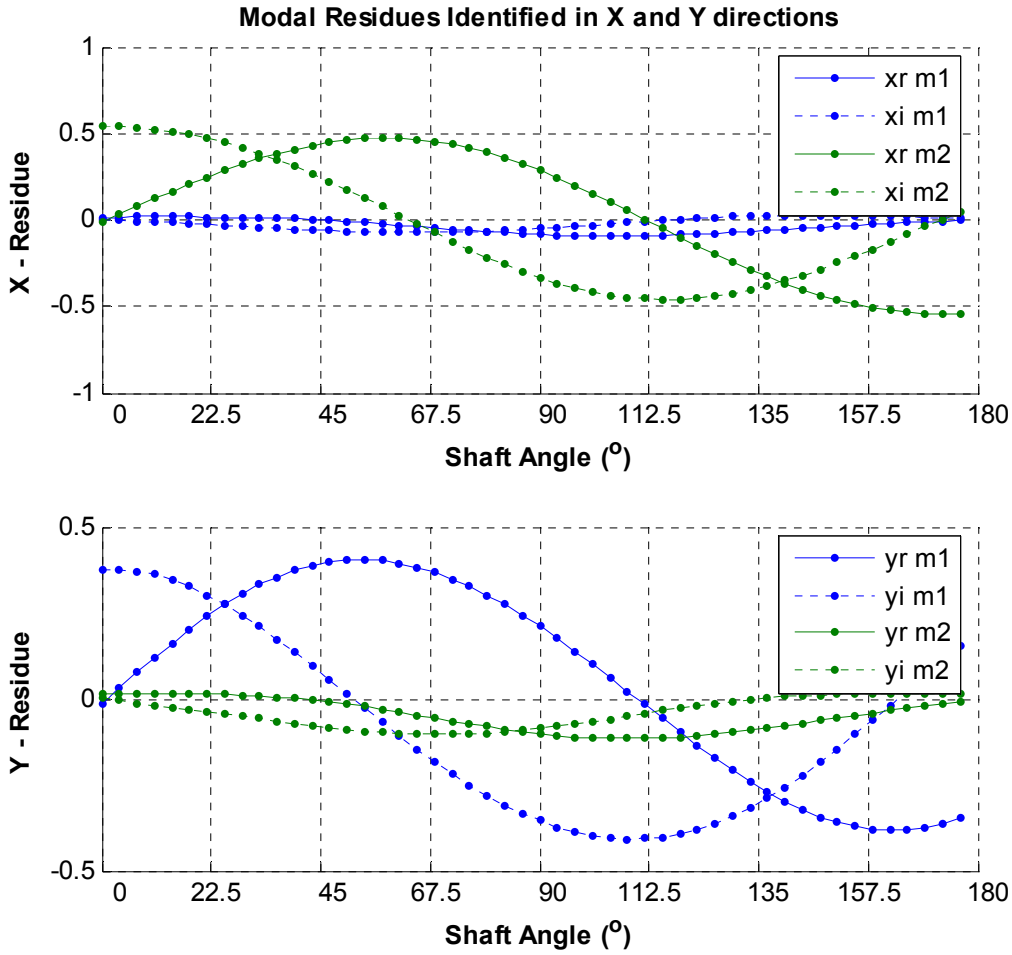

Figure 11: Residues identified by AMI from the collection of LTI systems (Method #1).

The residues in Figure 11 appear to vary strongly with shaft angle, yet this variation is a consequence of the fact that the response of each LTI system to which the residues belong begins at a different initial time. To remedy this, we appeal to the summation form of the Floquet representation of the response in eq. (11). Applying the initial conditions to eq. (11), the impulse response in terms of the modal parameters follows.

$$x(t) = \sum_{r=1}^{2N} \left(A_R\right)_r \exp\left(\lambda_r (t - t_0)\right)\left\{x(t_0)\right\} \qquad (17).$$

The responses at time instants separated by T_A, which are processed by using Method #1, follow.

$$
\begin{aligned}
x(nT_A + t_0) &= \sum_{r=1}^{2N} \left(A_R(t_0)\right)_r \exp\left(\lambda_r (nT_A - t_0)\right)\{x(t_0)\} \\
x(nT_A + t_1) &= \sum_{r=1}^{2N} \left(A_R(t_1)\right)_r \exp\left(\lambda_r (nT_A - t_1)\right)\exp\left(\lambda_r (t_1 - t_0)\right)\{x(t_0)\} \\
x(nT_A + t_2) &= \sum_{r=1}^{2N} \left(A_R(t_2)\right)_r \exp\left(\lambda_r (nT_A - t_2)\right)\exp\left(\lambda_r (t_2 - t_0)\right)\{x(t_0)\} \\
&\dots
\end{aligned}
\qquad (18),
$$

The strategy in Method #1 is to process these responses globally, as if they resulted from a single LTI system. As a result, the identification routine finds the following representation for the impulse response:

$$
\begin{aligned}
x(nT_A + t_0) &= \sum_{r=1}^{2N} \left(A_{Ident}\right)_r \exp\left(\lambda_r (nT_A - t_0)\right)\{x(t_0)\} \\
x(nT_A + t_1) &= \sum_{r=1}^{2N} \left(A_{Ident}\right)_r \exp\left(\lambda_r (nT_A - t_1)\right)\{x(t_0)\} \\
x(nT_A + t_2) &= \sum_{r=1}^{2N} \left(A_{Ident}\right)_r \exp\left(\lambda_r (nT_A - t_2)\right)\{x(t_0)\} \\
&\dots
\end{aligned}
\qquad (19),
$$

Comparing eq. (18) and (19) reveals that the residues identified via Method #1 for various initial times t_i are related to the true residues as follows.

$$\left(A_{Ident}\right)_{r,i} = \left(A_R(t_i)\right)_r \exp\left(\lambda_r (t_i - t_0)\right) \qquad (20),$$

If the Floquet eigenvalues are known, it is trivial to solve for the Floquet residues, which are denoted A_{Zero} because they (for all i) relate to the same initial condition at t_0.

$$\left(A_{zero}\right)_{r,i} = \left(A_{Ident}\right)_{r,i} \exp\left(-\lambda_r (t_i - t_0)\right) \qquad (21).$$

6. Acknowledgements

The authors would like to thank Ben Wagner for providing the initial motivation for this work and for his insights into the practical aspects of condition monitoring. This work was performed in part at Sandia National Laboratories and supported by the US Department of Energy under contract DE-AC04-94AL85000.

References

[1] G. Floquet, "Sur les Equations Lineaires a Coefficients Periodiques," *Ann. Sci. Ecole Norm. Sup.*, vol. 12, pp. 47-88, 1883.

[2] J. A. Richards, *Analysis of Periodically Time-Varying Systems*: Springer-Verlag, Berlin, Heidelberg, New York, 1983.

[3] P. Montagnier, R. J. Spiteri, and J. Angeles, "The Control of Linear Time-Periodic Systems Using Floquet-Lyapunov Theory," *International Journal of Control*, vol. 77, pp. 472-490, 2004.

[4] P. Friedmann, C. E. Hammond, and T.-H. Woo, "Efficient Numerical Treatment of Periodic Systems with Application to Stability Problems," *International Journal for Numerical Methods in Engineering*, vol. 11, pp. 1117-1136, 1977.

[5] G. Bir and K. Stol, "Operating Modes of a Teetered-Rotor Wind Turbine," presented at 17th International Modal Analysis Conference (IMAC XVII), Kissimmee, Florida, 1999.

[6] F. Oncescu, A. A. Lakis, and G. Ostiguy, "Investigation of the Stability and Steady State Response of Asymmetric Rotors, Using Finite Element Formulation," *Journal of Sound and Vibration*, vol. 245, pp. 303-328, 2001.

[7] Y. M. Fu and Y. F. Zheng, "Analysis of Non-Linear Dynamic Stability for A Rotating Shaft-Disk with Atransverse Crack," *Journal of Sound and Vibration*, vol. 257, pp. 713–731, 2002.

[8] G. T. Flowers, D. B. Margithu, and G. Szasz, "The Application of Floquet Methods in the Analyses of Rotordynamic Systems," *Journal of Sound and Vibration*, vol. 218, pp. 249-259, 1998.

[9] H. A. DeSmidt, K. W. Wang, and E. C. Smith, "Coupled Torsion-Lateral Stability of a Shaft-Disk System Driven Through a Universal Joint," *Journal of Applied Mechanics*, vol. 69, pp. 261-273, 2002.

[10] S. C. Sinha and R. Pandiyan, "Analysis of Quasilinear Dynamical Systems with Periodic Coefficients via Liapounov-Floquet Transformation," *International Journal of Non-Linear Mechanics*, vol. 29, pp. 687-702, 1994.

[11] J. S. Bendat and A. G. Piersol, *Engineering Applications of Correlation and Spectral Analysis*. New York: Wiley, 1980.

[12] B. Peeters and G. De Roeck, "Reference Based Stochastic Subspace Identification for Output-Only Modal Analysis," *Mechanical Systems and Signal Processing*, vol. 13, pp. 855-878, 1999.

[13] P. Van Overschee and B. De Moor, *Subspace Identification for Linear Systems: Theory-Implementation-Applications*. Boston: Kluwer Academic Publishers, 1996.

[14] H. Van Der Auweraer, P. Guillame, P. Verboven, and S. Vanlaunduit, "Application of a Fast-Stabilizing Frequency Domain Parameter Estimation Method," *Journal of Dynamic Systems, Measurement, and Control*, vol. 123, pp. 651-658, 2001.

[15] M. S. Allen, "Global and Multi-Input-Multi-Output (MIMO) Extensions of the Algorithm of Mode Isolation (AMI)," in *George W. Woodruff School of Mechanical Engineering*. Atlanta, Georgia: Georgia Institute of Technology, 2005, pp. 129.

[16] M. S. Allen and J. H. Ginsberg, "SIMO Extension of the Algorithm of Mode Isolation," presented at IMAC 22 - XXII International Modal Analysis Conference, Dearborn, Michigan, 2004.

[17] M. S. Allen and J. H. Ginsberg, "A Global, Single-Input-Multi-Output (SIMO) Implementation of The Algorithm of Mode Isolation and Applications to Analytical and Experimental Data," *Mechanical Systems and Signal Processing*, vol. Under Review, 2005.

[18] M. S. Allen and J. H. Ginsberg, "Global, Hybrid, MIMO Implementation of the Algorithm of Mode Isolation," presented at 23rd International Modal Analysis Conference (IMAC XXIII), Orlando, Florida, 2005.

[19] S. C. Sinha and V. Juneja, "An Approximate Analytical Solution for Systems With Periodic Coefficients via Symbolic Computation," presented at AIAA/ASME/ASCE/AHS/ACS 32ND Structures, Structural Dynamics, And Materials Conference, Baltimore, MD, 1991.

[20] S. C. Sinha, E. Gourdon, and Y. Zhang, "Control of time-periodic systems via symbolic computation with application to chaos control," *Communications in Nonlinear Science and Numerical Simulation*, vol. 10, pp. 835-854, 2005.